Multiferroics

DOI: 10.1002/ange.201202848

Multiferroics by Rational Design: Implementing Ferroelectricity in Molecule-Based Magnets**

Emilio Pardo, Cyrille Train, Hongbo Liu, Lise-Marie Chamoreau, Brahim Dkhil, Kamal Boubekeur, Francesc Lloret, Keitaro Nakatani, Hiroko Tokoro, Shin-ichi Ohkoshi, and Michel Verdaguer**

Multiferroics (MF) are materials that exhibit simultaneously several ferroic order parameters. Among the multiferroic materials, those combining antiferro- or ferroelectricity (FE) and antiferro-, ferri-, or ferromagnetism (FM) within the same material are highly desirable: the coexistence of the polar and magnetic orders paves the way towards four-level memories while their interactions through the magnetoelectric effect makes it possible to control the magnetization by electric fields and hence to develop electronically tuneable magnetic devices, which are an essential feature for spintronics.[1] Given the vicinity of solid-state chemistry and physics, oxides are the most studied MF, both as bulk materials and thin films.[2] Perovskite oxides of the general formula ABO_3 form the most extensively studied family because they comprise numerous ferroelectric and ferromagnetic materials. Nevertheless, the occurrence of FE and FM cannot rely on a single metal ion because, in such oxides, FE is related to the mobility of the metal ions within its oxygen coordination spheres,[3a] which is hindered by the presence of unpaired electrons necessary for the appearance of FM. This limitation has been somehow by-passed by choosing a second metal ion possessing a lone pair or by introducing charge ordering but the number of possible materials is still severely restricted.[1b]

Molecular materials can offer an appealing alternative route towards multiferroic compounds.[3b,c] Exchange interactions between bridged metal ions are well understood and led already to the design of room-temperature ferromagnetic molecular materials as observed in Prussian blue analogs (PBA).[4] In previous attempts to obtain molecular multiferroics, compounds exhibiting one of the two expected properties were revisited to find out whether they could have the second property as well.[5]

We propose an alternative strategy that uses from the beginning the versatility of inorganic–organic hybrid materials to address the expected properties of multiferroic materials.[6a,b] The basis of our approach is the well-established hosting behavior and the magnetic properties of oxalate-bridged bimetallic two-dimensional (2D) networks[6a,c] (Scheme 1) coupled to the referenced ferroelectric properties of 4-aminopyridinium salts.[7] We thus obtained $C[MnCr(ox)_3(CH_3CH_2OH)]$ (**1**) (C^+ = 1-(hydroxyethyl)-4-(*N*,*N*-dimethylamino)pyridinium; $ox^{2-} = C_2O_4^{2-}$). The structure of this material combines a 2D oxalate-based bimetallic

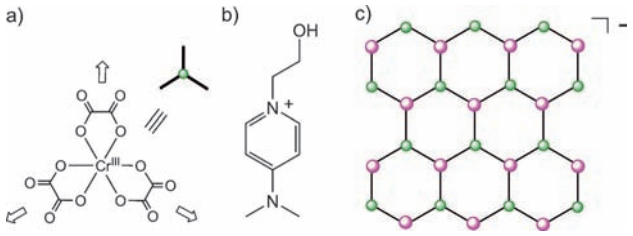

Scheme 1. Metal ligand design strategy of **1** using a) the tris(bidentate) mononuclear chromium(III) complex anion as molecular tecton with b) a pyridinium-based polar cation, c) leading to the formation of 2D bimetallic oxalate-bridged layers.

[*] Dr. E. Pardo, L.-M. Chamoreau, Prof. Dr. K. Boubekeur, Prof. Dr. M. Verdaguer
Institut Parisien de Chimie Moléculaire, UMR CNRS 7201 UPMC-Univ. Paris 06
4 place Jussieu, 75252 Paris CEDEX 05 (France)
E-mail: michel.verdaguer@upmc.fr
Prof. Dr. C. Train
Laboratoire National des Champs Magnétiques Intenses UPR CNRS 3228, B.P. 166, 38042 Grenoble cedex 9 (France)
and
Université Joseph Fourier, BP 53, 38041 Grenoble Cedex 9 (France)
Institut Universitaire de France (IUF)
E-mail: cyrille.train@lncmi.cnrs.fr
H. Liu, Dr. B. Dkhil
Laboratoire Structures, Propriétés et Modélisation des Solides, CNRS-UMR 8580 Ecole Centrale Paris
Paris, 92295 Châtenay-Malabry cedex (France)
Dr. E. Pardo, Prof. Dr. F. Lloret
Departament de Química Inorgànica, Instituto de Ciencia Molecular (ICMOL), Universitat de València
46980 Paterna, València (Spain)
Prof. Dr. K. Nakatani
PPSM (UMR CNRS 8531), Institut d'Alembert (IFR 121, FR 3242)
Ecole Normale Supérieure de Cachan, 94235 Cachan (France)
Dr. H. Tokoro, Prof. Dr. S. Ohkoshi
Department of Chemistry, School of Science
The University of Tokyo
7-3-1 Hongo, Bunkyo-ku, Tokyo 113-0033 (Japan)

[**] This work was supported by the Centre National de la Recherche Scientifique (CNRS, France), the Ministère de l'Enseignement Supérieur et de la Recherche (MESR, France), the Agence Nationale de la Recherche (ANR, France; project number ANR-08-JCJC-0113-01), the MICINN (Spain, project numbers CTQ2010-15364 and CSD2007-00010). PRES UniverSud is acknowledged for its support for SHG equipment. E.P. and C.T. acknowledge the MEC and the Japan Society for the Promotion of Science (JSPS) for their postdoctoral grants.

Supporting information for this article is available on the WWW under http://dx.doi.org/10.1002/anie.201202848.

anionic network and polar stacks of cations. The host anionic network provides long-range ferromagnetic ordering whereas the counterions give rise to ferroelectric properties.

The synthesis of **1** relies on the versatility of molecular chemistry. Instead of 4-(*N*,*N*-dimethylamino)pyridinium,[7] we have selected 1-(hydroxyethyl)-4-(*N*,*N*-dimethylamino)pyridinium (C^+, Scheme 1b) 1) to favor the formation of an extended coordination network over discrete polynuclear complexes[8] and 2) to introduce a complementary polar moiety and increase the possibility of hydrogen bonds, known to play a central role in the appearance of FE.[3b,7] The synthesis of this new cation was achieved by a nucleophilic substitution of the iodine atom of 2-iodoethanol by 4-(*N*,*N*-dimethylamino)pyridine. The formation of **1** is insured by using tris(oxalato)chromate(III) building blocks as metal-containing ligands towards manganese(II) ions resulting in the formation of an anionic coordination network, the charge of which is compensated by the insertion of C^+. A metathesis of the ammonium cation by C^+ in the tris(oxalato)chromate-(III) precursor salt leads to the formation of **1** rather than $(NH_4)_4[MnCr_2(ox)_6]\cdot 4H_2O$ which also crystallizes from water/alcohol mixtures.[6d]

The crystal structure of **1** has been determined by single-crystal X-ray diffraction. Compound **1** crystallizes in the orthorhombic system, polar space group $P\,na2_1$ between 100 and 350 K, where it loses its crystallinity because of solvent loss. The structure consists of bimetallic, anionic $[MnCr(ox)_3(C_2H_5OH)]^-$ corrugated sheets lying in the *ac* plane which are interleaved by stacks of 1-(hydroxyethyl)-4-(*N*,*N*-dimethylamino)pyridinium cations running along the *a* axis (Figures 1 and 2 and Figures S1 and S2 in the Supporting Information). Within the layers, the chromium(III) ion is coordinated to six oxygen atoms from three oxalate ligands, building a trigonally distorted octahedron. The manganese(II) ion is surrounded by seven oxygen atoms from three oxalate ligands with Mn–O distances found between 2.1696(8) and 2.5375(8) Å at 110 K, and by a coordinated ethanol molecule. The geometry around the heptacoordinated manganese(II) appears as an heavily distorted pentagonal bipyramid (Figure 1a and Figure S1). The tris(oxalato)chromate(III) tecton, used here as a stable metal-containing ligand is similar to those reported in other 2D oxalate-based compounds.[6] Both metal ions behave as triconnectors and the 2D coordination network presents the usual (6,3)net topology[6e] and a honeycomb-like organization (Figure 1a). Nevertheless, the distortion of the Mn^{II} coordination sphere related to the presence of the ethanol molecule and the interactions with the cation induce a distortion and a strong corrugation of the bimetallic layers (Figure 1) though it does not reach the quasi-brick-wall character already observed[6f] when the distortion of the manganese(II) coordination environment is larger. The stacking of the successive layers along the *b* axis builds egg-shaped pockets wrapping the C^+ cation (Figure 1b).

1-(Hydroxyethyl)-4-(*N*,*N*-dimethylamino)pyridinium cations are organized in columns where the cations are π-stacked along the *a* axis (Figure 1b). Two neighboring molecules along this axis are staggered by 48.76 degrees. The mean direction of their longer axis is aligned along *c*, parallel to the oxalate layers, all the amino groups pointing in the same direction. There are many close contacts between the hydrogen atoms of the cations and the anionic network (Figure 2a). Among them, there are two types of H bonds (Figure 2a): 1) The oxygen atoms of the 1-(hydroxyethyl)-4-(*N*,*N*-dimethylamino)pyridinium cations form O−H···O bonds with the oxalate oxygen atoms [O14···O12 = 3.0780(14) Å and O14···O5 = 3.0293(14) at 110 K], and 2) carbon-oxygen hydrogen bonds are also found [C···O = 3.2228(18)–3.5142(15) Å at 110 K]; the shorter bonds are found between neighboring cations (see Figure S2). The molecular $(N1)^+$-O14 dipolar electric moments combine and create an overall dipolar moment with a strong component along the *c* axis (Figure 2b). The organization of the polar cations in **1** is reminiscent of the polar phase of $[4\text{-}NH_2C_5H_4NH][SbCl_4]$, at the origin of its ferroelectric behavior.[7]

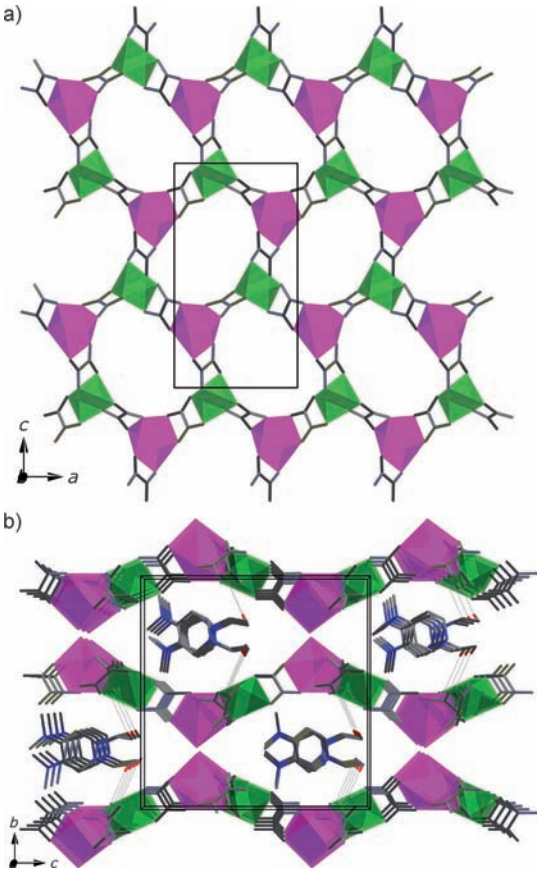

Figure 1. X-ray crystal structure of **1** at 110 K. a) Anionic network of **1** in the *ac* plane. b) Packing of the cations between the corrugated planes. The Cr and Mn atoms are depicted as green and purple polyhedra, respectively. Oxygen, hydrogen, and nitrogen atoms are given in red, pink, and blue, respectively. The hydrogen bonds are given by dashed lines.

When compared to the structure of most common 2D oxalate-based bimetallic networks, **1** shows a strong structural synergy between the cation and the coordination network. Two remarkable observations are the lengthening of the Mn1–O12 distance associated to the O14–H14···O12 hydrogen bond and the polar organization of the cations.

The magnetic properties of **1** are displayed in Figure S3 in a plot of $\chi_M T$ versus T, where χ_M is the molar magnetic

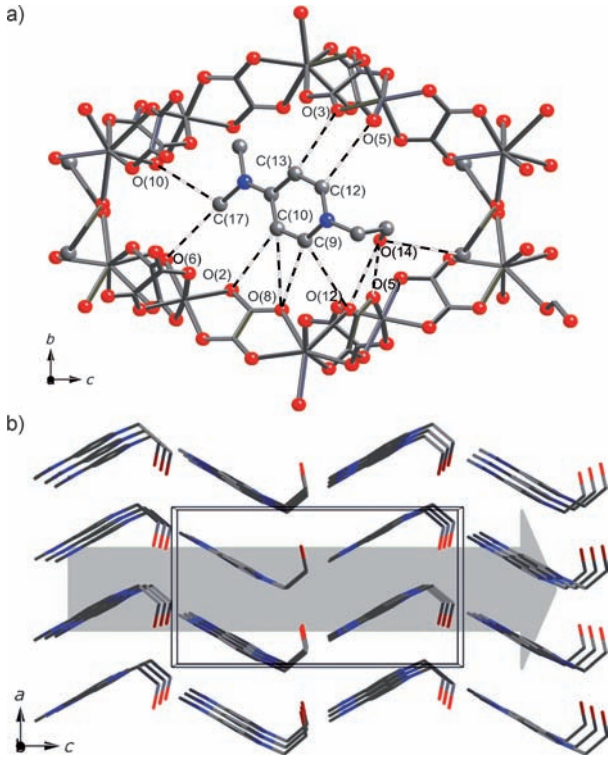

Figure 2. a) Fragment of **1** in the *bc* plane, emphasizing the O–H···O and C–H···O hydrogen bonds. b) Organization of the 1-(hydroxyethyl)-4-(*N*,*N*-dimethylamino)pyridinium polar cations in the *ac* plane; the polar arrangement of the guest molecules is emphasized by the grey arrow.

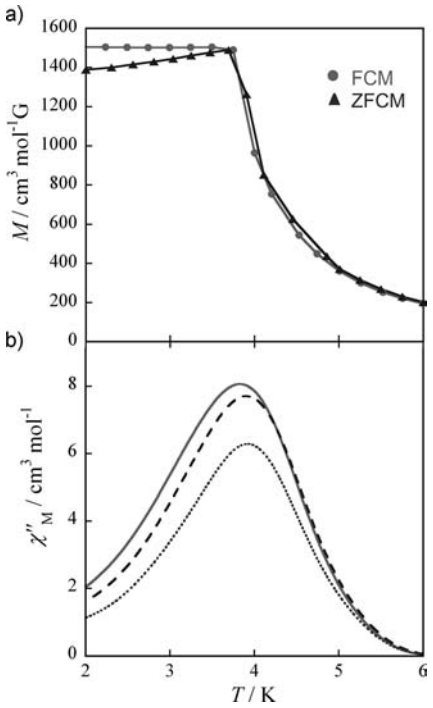

Figure 3. a) Field-cooled magnetization (FCM) and zero-field-cooled magnetization (ZFCM) of **1**. b) Temperature dependence of the ac out-of-phase magnetic susceptibility of **1** at frequencies of 10 Hz (dotted line), 100 Hz (dashed line), and 900 Hz (solid line).

susceptibility per MnCr unit and T is the temperature. At room temperature, the $\chi_M T$ value is 6.37 $cm^3 mol^{-1} K$. This is slightly larger than expected for the sum of the $\chi_M T$ values of one Cr^{III} ion and one high-spin Mn^{II} ion with $g_{Cr} = g_{Mn} = 2.00$. Upon cooling, $\chi_M T$ increases at a continuously increasing rate to reach a maximum value of $\chi_M T$ of 80.6 $cm^3 mol^{-1} K$ at 4 K. Both observations suggest a moderate ferromagnetic interaction between the Mn^{II} and Cr^{III} ions through the oxalate bridge. Such parallel alignment of the neighboring local spins is well documented.[8]

The compound undergoes an abrupt paramagnetic-to-ferromagnetic phase transition at $T_C = 3.9$ K (Figure 3). The ferromagnetic ordering is revealed by the coalescence of the field-cooled magnetization (FCM) and the zero-field-cooled magnetization (ZFCM) curves at 3.9 K (Figure 3a). The ferromagnetic ordering is confirmed by the alternating current (ac) magnetic measurements because the out-of-phase magnetic susceptibility becomes nonzero below 6 K and shows frequency-independent maxima around 4.0 K (Figure 3b). Finally this magnetic ordering results in the typical λ peak observed for specific heat capacity measurements (Figure S4). Ferromagnetic order is often observed in oxalate-based 2D [MnCr] compounds with nondistorted Cr–oxalate–Mn bridges. An exception is the ferrimagnetic ordering observed in $[Mn(OCH_3)_6][MnCr(ox)_3(CH_3OH)]_2$ because of the antiferromagnetic exchange interaction between the two metal ions attributed to a very long Mn–O [2.811(4) Å] distance.[6f] In **1**, with a smaller distortion of the oxalate bridge, the exchange interaction remains ferromagnetic (Figure 3 and Figure S3 in the Supporting Information) but the Curie temperature is slightly lower than those temperatures observed in regular [MnCr] networks.[6g,9a]

The polar alignment of C^+ cations (Figure 2b) together with the aforementioned H-bonding interactions (Figure 2a) and the spatial asymmetry, are key factors for the appearance of ferroelectric properties. The polar space group determined for **1** is associated with a non-centrosymmetric point group mm2 (C_{2v}). This point group allows the observation of FE as well as second harmonic generation (SHG).[9b] The symmetry requirements for SHG are less restrictive than those for FE and SHG does not require cooperative interactions as those needed for FE. For example, $[NCH_3(CH(CH_3)C_2H_5)(C_3H_7)_2][MnCr(ox)_3]$ fulfills the symmetry requirements for observing SHG and FE.[9a] Experimentally, this complex exhibits SHG properties,[9c] but no FE properties were observed. Since SHG measurements do not require electrical contacts, they can be used as a preliminary diagnosis of the presence of FE.[10] The SHG efficiency of **1** is up to 10–15 times that of urea at 1.9 μm. This efficiency and the polar character of the C^+ cations makes FE in **1** likely.

The electric properties of **1** have thus been investigated thoroughly (Figure 4 and Figure S5). To distinguish the conduction properties from FE,[11a] the temperature dependence of the direct current (dc) resistivity was first investigated. The resistivity strongly increases when the temperature decreases (Figure 4a) showing that **1** is a wide-bandgap semiconductor (SC). An Arrhenius analysis reveals an

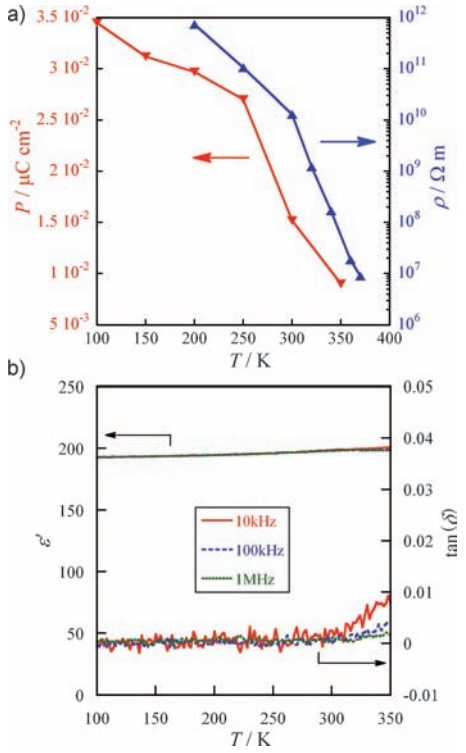

Figure 4. Temperature dependence of a) the remnant electric polarization (left) and the dc resistivity (right) and b) the dielectric permittivity ε′ (left) and the dielectric losses tan(δ) (right) of **1** at different frequencies.

activation energy of about 1 eV for the charge carriers. This value is similar to the value obtained for multiferroic materials such as $BiFeO_3$.[11b] After the SC behavior of **1** had been established, ac measurements were performed between 100 and 350 K to determine the electric polarization (Figure 4a and Figure S5) as well as the dielectric permittivity and dielectric losses (Figure 4b) of **1**. From 10 kHz up to 10 MHz, the complex impedance of the compound shows a phase close to 90° in the whole temperature range. This feature indicates that the capacitive properties of **1** dominate the resistive properties in this frequency range. Modeling the sample at lower frequencies by an equivalent electric circuit composed of a capacitor and a resistance in parallel arrangement makes it possible to extract the capacitive contribution quantitatively. When the temperature decreases, the remnant (Figure 4a) and saturation polarizations (Figure S5) increase. When the temperature decreases, the enhancement of the signal together with a concomitant increase of the resistivity mentioned above indicate that an intrinsic polarization of **1** is indeed observed, establishing its ferroelectric behavior. At 100 K, the remnant polarization is 0.035 $\mu C\,cm^{-2}$ whereas the saturation value is 0.070 $\mu C\,cm^{-2}$. This value is close to the value reported for the parent 4-aminopyridinium salt.[7,12] The value is comparable to values of other extensively studied multiferroics like $TbMnO_3$ or $TbMn_2O_5$ and larger than those values of many other materials.[13] In relation to the appearance of electric polarization, the cigar shape of the loops (see Figure S5) is typical of lossy dielectrics or soft ferroelectrics.[5a,11d,e] The dielectric constant ε′ is as high as about 200 whereas the dielectric losses remain low with tan(δ) values below 0.01 (Figure 4b). Moreover, they are remarkably stable to temperature. These measurements indicate that **1** is a ferroelectric material within the whole temperature range explored. The absence of a ferroelectric-to-paraelectric phase transition between 100 and 350 K indicates that the ferroelectric Curie point of **1** should be found above 350 K, that is, at a temperature at which decomposition of the compound or loss of solvent is likely.[11c] Because of the intermolecular interactions between the anionic network and the cation, formation of hydrogen bonds involving the O14-H14 unit as, for example, in O-H···O and O···H-O, is more likely to explain the ferroelectric behavior of **1** than the rotation of the entire polar molecule within the network cavity.

In conclusion, we have successfully used two interpenetrating networks to design and synthesize a molecular multiferroic hybrid material based on molecular precursors which are known to favor ferromagnetic and ferroelectric properties. Self-assembly has led to a structure in which the 2D oxalate-bridged bimetallic corrugated layers wrap the organic cations within a space group compatible with second harmonic generation, ferromagnetism, and ferroelectricity. The coordination network yields a ferromagnetic ordering at low temperatures whereas the influence of the high-frequency electric field on the polar cations leads to a ferroelectric behavior within the whole temperature range explored. Although the ferromagnetic Curie temperature and the electrical polarization are still weak and the observation of the magnetoelectric effect remains a challenge, this approach shows that efficient multiferroics with ferromagnetic order can be obtained by rational design. This approach leads to multiferroics with much higher magnetization relative to ordinary multiferroics with spiral or canted antiferromagnetic orders. This molecular strategy is applicable to bulk materials but also, through layer-by-layer approaches,[14] to nanostructured materials which can be used in molecular devices.[15]

Received: April 13, 2012
Revised: June 22, 2012
Published online: July 5, 2012

Keywords: chromium · manganese · molecular magnets · multiferroics

[1] a) W. Eerenstein, N. D. Mathur, J. F. Scott, *Nature* **2006**, *442*, 759–765; b) S. W. Cheong, M. Mostovoy, *Nat. Mater.* **2007**, *6*, 13–20; c) D. Khomskii, *Physics* **2009**, *2*, 20.
[2] R. Ramesh, N. A. Spaldin, *Nat. Mater.* **2007**, *6*, 21.
[3] a) N. A. Hill, *J. Phys. Chem. B* **2000**, *104*, 6694–6709; b) S. Horiuchi, Y. Tokura, *Nat. Mater.* **2008**, *7*, 357–366; c) T. Akutagawa, H. Koshinaka, D. Sato, S. Takeda, S.-I. Noro, H. Takahashi, R. Kumai, Y. Tokura, T. Nakamura, *Nat. Mater.* **2009**, *8*, 342–347.
[4] S. Ferlay, T. Mallah, R. Ouahes, P. Veillet, M. Verdaguer, *Nature* **1995**, *378*, 701–703.
[5] a) S. Ohkoshi, H. Tokoro, T. Matsuda, H. Takahashi, H. Irie, K. Hashimoto, *Angew. Chem.* **2007**, *119*, 3302–3305; *Angew. Chem. Int. Ed.* **2007**, *46*, 3238–3241; b) P. Jain, V. Ramachandran, R. J. Clark, H. D. Zhou, B. H. Toby, N. S. Dalal, H. W. Kroto, A. K.

Cheetham, *J. Am. Chem. Soc.* **2009**, *131*, 13625 – 13627; c) G. Rogez, N. Viart, M. Drillon, *Angew. Chem.* **2010**, *122*, 1965 – 1967; *Angew. Chem. Int. Ed.* **2010**, *49*, 1921 – 1923; d) A. Stroppa, P. Jain, P. Barone, M. Marsman, J. M. Perez-Mato, A. K. Cheetham, H. W. Kroto, S. Picozzi, *Angew. Chem.* **2011**, *123*, 5969 – 5972; *Angew. Chem. Int. Ed.* **2011**, *50*, 5847 – 5850; e) G.-C. Xu, W. Zhang, X.-M. Ma, Y.-H. Chen, L. Zhang, H.-L. Cai, Z.-M. Wang, R.-G. Xiong, S. Gao, *J. Am. Chem. Soc.* **2011**, *133*, 14948 – 14951; f) D.-W. Fu, W. Zhang, H.-L. Cai, Y. Zhang, J.-Z. Ge, R.-G. Xiong, S. D. Huang, T. Nakamura, *Angew. Chem.* **2011**, *123*, 12153 – 12157; *Angew. Chem. Int. Ed.* **2011**, *50*, 11947 – 11951; g) A. O. Polyakov, A. H. Arkenbout, J. Baas, G. R. Blake, A. Meetsma, A. Caretta, P. H. M. Loosdrecht, T. T. M. Palstra, *Chem. Mater.* **2012**, *24*, 133 – 139.

[6] a) M. Clemente-León, E. Coronado, C. Martí-Gastaldo, F. M. Romero, *Chem. Soc. Rev.* **2011**, *40*, 473 – 497; b) C. Train, M. Gruselle, M. Verdaguer, *Chem. Soc. Rev.* **2011**, *40*, 3297 – 3312; c) R. Clément, S. Decurtins, M. Gruselle, C. Train, *Monatsh. Chem.* **2003**, *134*, 117 – 135; d) E. Pardo, C. Train, G. Gontard, K. Boubekeur, O. Fabelo, H. Liu, B. Dkhil, F. Lloret, K. Nakagawa, H. Tokoro, S. Ohkoshi, M. Verdaguer, *J. Am. Chem. Soc.* **2011**, *133*, 15328 – 15331; e) M. Gruselle, C. Train, K. Boubekeur, P. Gredin, N. Ovanesyan, *Coord. Chem. Rev.* **2006**, *250*, 2491 – 2500; f) E. Coronado, J. R. Galán-Mascarós, C. Martí-Gastaldo, A. Murcia-Martínez, *Dalton Trans.* **2006**, 3294 – 3299; g) M. Gruselle, R. Andres, B. Malezieux, M. Brissard, C. Train, M. Verdaguer, *Chirality* **2001**, *13*, 712 – 714.

[7] R. Jakubas, Z. Ciunik, G. Bator, *Phys. Rev. B* **2003**, *67*, 024103.

[8] E. Pardo, C. Train, R. Lescouëzec, K. Boubekeur, E. Ruiz, F. Lloret, M. Verdaguer, *Dalton Trans.* **2010**, *39*, 4951 – 4958.

[9] a) C. Train, R. Gheorghe, V. Krstic, L.-M. Chamoreau, N. S. Ovanesyan, G. L. J. A. Rikken, M. Gruselle, M. Verdaguer, *Nat. Mater.* **2008**, *7*, 729 – 734; b) K. M. Ok, E. O. Chi, P. S. Halasyamani, *Chem. Soc. Rev.* **2006**, *35*, 710 – 717; c) C. Train, T. Nuida, R. Gheorghe, M. Gruselle, S. Ohkoshi, *J. Am. Chem. Soc.* **2009**, *131*, 16838 – 16843.

[10] W. Zhang, R.-G. Xiong, *Chem. Rev.* **2012**, *112*, 1163 – 1195.

[11] a) MF often exhibit leakage currents (electronic conduction) that can affect polarization measurements; b) G. Catalan, J. F. Scott, *Adv. Mater.* **2009**, *21*, 2463 – 2485; c) N. Leblanc, N. Mercier, L. Zorina, S. Simonov, P. Auban-Senzier, C. Pasquier, *J. Am. Chem. Soc.* **2011**, *133*, 14924 – 14927; d) J. F. Scott, *J. Phys. Condens. Matter* **2008**, *20*, 021001; e) J. Hemberger, P. Lunkenheimer, R. Fichtl, H.-A. Krug von Nidda, V. Tsurkan, A. Loidl, *Nature* **2005**, *434*, 364 – 367.

[12] The polarization value of **1** is actually about ten times lower than that one reported in Ref. [7]. This discrepancy is explained by 1) the technique used in Ref. [7], namely the integration of a pyroelectric current, which includes the leaky charges (the reported losses $\tan(\delta) < 0.1$ in Ref. [13] are higher than the losses reported for **1**) and 2) also by the fact that the polarization was measured along the main polar axis in Ref. [13] while the small size of the as-grown crystals of **1** did not allow for such measurements.

[13] a) T. Kimura, T. Goto, H. Shintani, K. Ishizaka, T. Arima, Y. Tokura, *Nature* **2003**, *426*, 55 – 58; b) N. Hur, S. Park, P. A. Sharma, J. S. Ahn, S. Guha, S.-W. Cheong, *Nature* **2004**, *429*, 392 – 395; c) K. F. Wang, J. M. Liu, Z. F. Ren, *Adv. Phys.* **2009**, *58*, 321 – 448.

[14] G. Molnár, S. Cobo, J. A. Real, F. Carcenac, E. Daran, C. Vieu, A. Bousseksou, *Adv. Mater.* **2007**, *19*, 2163 – 2167.

[15] M. Bibes, J. E. Villegas, A. Barthélémy, *Adv. Phys.* **2011**, *60*, 5 – 84.

